Available online at www.sciencedirect.com
ScienceDirect
Nuclear Physics B Proceedings Supplement 00 (2014) 1–5
Nuclear Physics B Proceedings Supplement

# Minimum Bias, MPI and DPS, Diffractive and Exclusive measurements at CMS

Dipanwita Dutta on behalf of CMS Collaboration

*Nuclear Physics Division, Bhabha Atomic Research Centre, Mumbai-400085, India.*

**Abstract**

We present recent results on Minimum Bias, MPI and DPS, Diffractive and Exclusive studies using data collected during Run 1 of the LHC. The measurements include data collected in pp collisions at $\sqrt{s} = 7$, and 8 TeV by the CMS Collaboration. Double parton scattering is investigated in several final states including vector bosons and jets, and the effective cross section results are compared to other experiments and to MPI models tuned to recent underlying event measurements at CMS. Inclusive diffractive cross sections are discussed and compared to models, while searches and measurements of central exclusive processes are presented. The results from the first combined measurement by the CMS+TOTEM collaborations of the pseudorapidity distribution of charged particles at 8 TeV are also discussed, and are compared to models and to lower energy measurements.

*Keywords:* LHC, rapidity gaps, soft QCD, underlying events

## 1. Introduction

Forward, diffractive and exclusive physics cover a wide range of subjects, including low-x QCD, underlying event and multiple interactions characteristics, and central exclusive process. With excellent performance the Compact Muon Solenoid (CMS) experiment [1] has made a number of significant observations in diffractive and exclusive processes and hence to probe the Standard model in a unique way. The particle production in pp collisions at LHC, will allow to test the fundamental aspect of QCD, namely the interplay between soft and hard contributions to an interaction. Its good understanding is crucial for the proper modeling of the final state of Minimum-Bias events, and can help improve the simulation of e.g. the underlying event, pile-up events, and the measurement of the machine luminosity at the LHC. In this paper, we present the recent CMS results on diffraction, forward physics and soft QCD, and discuss their comparison to predictions of various theoretical models.

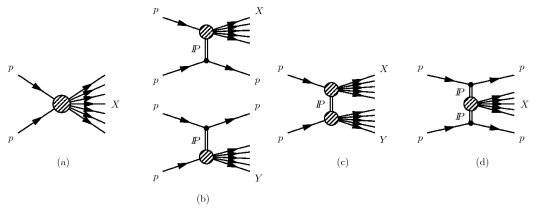


Figure 1: Schematic diagrams of (a) non-diffractive, $pp \to X$, and diffractive processes with (b) single dissociation, $pp \to Xp$ or $pp \to pY$, (c) double-dissociation, $pp \to XY$, and (d) central dissociation, $pp \to pXp$. The X(Y) represents a dissociated-proton or a centrally-produced hadronic system.

## 2. Diffractive processes

Diffractive interactions are characterized by the presence of at least one non-exponentially suppressed large rapidity gap (LRG) in the final state. LRG is defined as a region in pseudorapidity devoid of particles is presumed to be formed by a

color-singlet exchange with vacuum quantum numbers, referred to as Pomeron ($\mathbb{P}$) exchange. Inclusive (soft) diffractive interactions (with no hard scale) cannot be calculated within perturbative QCD (pQCD), and traditionally have been described by models based on Regge theory. Model predictions generally differ when extrapolated from pre-LHC energies (e.g. 1.96 TeV) to 7 TeV at LHC. Thus experimental results at LHC provide important input for tuning various models and current event generators. Fig. 1 shows the main types of diffractive processes: single dissociation (SD), double dissociation (DD) and central dissociation (CD).

Diffractive cross sections have been measured with CMS [2] using the low-pileup 2010 data of pp collision at $\sqrt{s} = 7$ TeV, corresponding to an integrated luminosity of 16.2 $\mu b^{-1}$. The SD and DD events were separated using the CASTOR calorimeter, which covers the very forward region of the experiment, $-6.6 < \eta < -5.2$. Minimum bias events were selected by requiring a signal above noise level in any of the BSC (Beam Scintillator Counter) devices ($3.2 < |\eta| < 4.7$) and the presence of at least two energy deposits in the central CMS detector ($|\eta| < 4.7$). Diffractive events were selected by requiring the presence of a forward rapidity gap reconstructed at the edge of the central detector or central gap. The forward gap on the positive (negative) side was reconstructed in terms of the variable $\eta_{max}$ ($\eta_{min}$) defined as the highest (lowest) $\eta$ of a particle reconstructed in the detector. The central gap was reconstructed as $\Delta\eta^0 = \eta^0_{max} - \eta^0_{min}$, with $\eta^0_{max}$ ($\eta^0_{min}$) defined as the closest-to-zero $\eta$ of a particle reconstructed on the positive (negative) $\eta$-side of the central detector, with an additional requirement of activity on both sides of the detector. The event sample after the $\eta_{min} > -1$ selection was used to extract SD and DD cross sections. Subsamples enhanced in SD and DD events were selected by requiring an absence or a presence of an energy deposit in the CASTOR calorimeter. The differential SD cross section as a function of $\xi$ (an incoming-proton momentum loss), and the differential DD cross section as a function of $\xi_X = M_X^2/s$ for $0.5 < \log_{10}(M_Y/GeV) < 1.1$ (CASTOR acceptance), after subtracting the background contribution to the signal (DD to SD and ND to DD), are shown in Fig. 2 (left) and (right), respectively. Results are compared to MC models.

The diffractive-event generation in MBR is based on a phenomenological renormalized Regge theory model [3]. The predictions of PYTHIA8-MBR are shown for two values of the parameter of the Pomeron trajectory $\alpha(t) = 1 + \epsilon + \alpha'(t)$, $\epsilon = 0.08$ and $\epsilon = 0.104$. Both values describe the measured SD cross section within uncertainties, while the DD data favor the smaller value of $\epsilon = 0.08$. The predictions of PYTHIA8-4C and PYTHIA6 describe well the measured DD cross section, but fail to describe the falling behavior of the data. The total measured SD cross section integrated over the region $5.5 < \log_{10}\xi < 2.5$ ($12 \leq M_X \leq 394$ GeV) is $\sigma^{SD}_{vis} = 4.27 \pm 0.04(stat.)^{+0.65}_{-0.58}(syst.)$ mb.

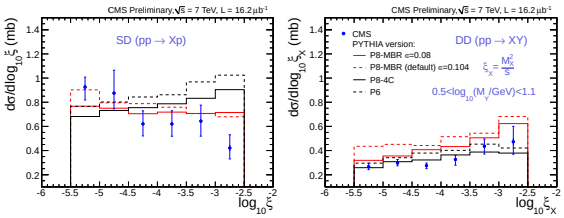


Figure 2: The SD (left) and DD (right) cross sections as a function of $\xi$ compared to PYTHIA6, PYTHIA8-4C and PYTHIA8-MBR MC predictions.

CMS with a close cooperation with TOTEM experiment, located at the same interaction point provides almost full coverage in pseudorapidities for charged and neutral particles. The CMS and TOTEM collaborations have measured [4] pseudorapidity distributions of charged particles, $dN_{ch}/d\eta$, using the low-pileup 2012 data at $\sqrt{s} = 8$ TeV ($L = 45\mu b^{-1}$), recorded during the common CMS and TOTEM runs with a non standard ($\beta^* = 90$m) LHC optics configuration. This is the first result of the combined CMS and TOTEM analysis, covering the ranges of $|\eta| < 2.2$ and $5.3 < |\eta| < 6.4$, respectively. Depending on the configuration of the T2 detectors with a signal, events were categorized into three different samples: (i) an inclusive sample, sensitive to $91 - 96\%$ of the total inelastic proton-proton cross section, (ii) a sample enhanced in non-single diffractive (NSD-enhanced) events, and (iii) a sample enhanced in single-diffractive (SD-enhanced) events. The measured $dN_{ch}/d\eta$ distributions for NSD-enhanced samples are presented in Fig. 3 showing that the charged particle density decreases with $\eta$. The results are compared to the predictions of various Monte Carlo models: PYTHIA6-Z2*, PYTHIA8-4C, HERWIG++, EPOS, and QGSJET-II-04. None of the models provides a consistent description of the measured distributions.

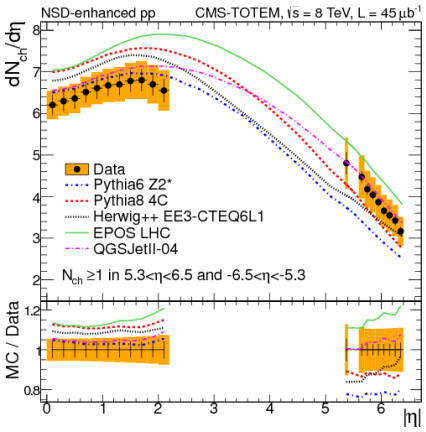


Figure 3: Charged-particle pseudorapidity distributions from a NSD-enhanced sample.

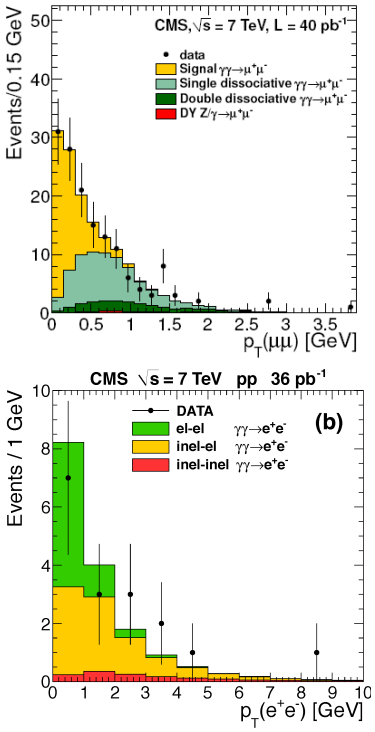


Figure 4: Muons (top) and electron (bottom) pairs transverse momentum distributions for the candidates selected in the two-photon production of leptons pairs.

## 3. Central Exclusive processes

Another class of processes with a LRG in the final state is central exclusive process (CEP). The CEP is a process of the type: $pp \to p + X + p$ with X being a well defined system e.g. di-lepton or di-jet. Exclusive means no additional activity between the outgoing protons and X, thus, the final state consists of the scattered protons which survive the interaction intact, and of the system X or its decay products. In the CEP, three distinct processes may be involved, namely photon-photon, photon-pomeron and pomeron-pomeron interactions. The system $X$ is reconstructed in the central CMS barrel, while forward detectors are used to veto non-exclusive events.

Exclusive di-lepton production $\gamma\gamma \to l^+l^-$ is a nearly pure QED process. Therefore its cross section is precisely known. Its measurement at the LHC is an independent cross check of the the absolute luminosity calibration [5, 6]. Two different di-lepton exclusive analyses have been performed using the data collected in 2010 at 7 TeV, namely for the measurements of $\gamma\gamma \to e^+e^-$ [5] and of $\gamma\gamma \to \mu^+\mu^-$ [6]. The event selection is requiring two leptons, which are energy or momentum balanced and back-to-back in the transverse plane. This corresponds to a $|p_T(l^+) - p_T(l^-)| < 1$ GeV as well as an acoplanarity describing the difference in azimuthal angles, $|1 - \Delta\phi(l^+, l^-)/\pi| < 0.1$.The dimuon analysis requires each of the two muons to carry a transverse momentum larger than 4 GeV in the range $|\eta(\mu)| < 2.1$. In order to reject the exclusive photoproduction of the low-mass resonances, an invariant mass cut is applied $M_{\mu^+\mu^-} > 11.5$ GeV.

For the dielectron analysis, a electron-positron pair with a transverse energy deposit in the calorimeters $E_T > 5.5$ GeV are selected in the range $|\eta(e)| < 2.5$. The selected sample consists of events of exclusive as well as semi-exclusive dilepton production, in which the dissociated proton escapes detection in the central detector. Fig. 4 shows the distributions of the $p_T$ of the di-muon pair (top) and di-electrton pair (bottom), and compared to LPAIR MC predictions for exclusive and semi-exclusive production. Good agreement between data and the simulation is observed. These two results allow to improve the understanding of this purely electromagnetic process, by observing 17 candidates for the dielectron channel and by a measurement of a production cross-section at $\sqrt{s} = 7$ TeV for the dimuon channel:

$$\sigma(pp \to p\mu^+\mu^- p) = 3.38^{+0.58}_{-0.55}(\text{stat.}) \pm 0.16(\text{syst.}) \pm 0.14(\text{lumi.})\ \text{pb}.$$

Several processes beyond the Standard model predict an anomalous quartic gauge coupling (AQGC) which can be translated into a higher

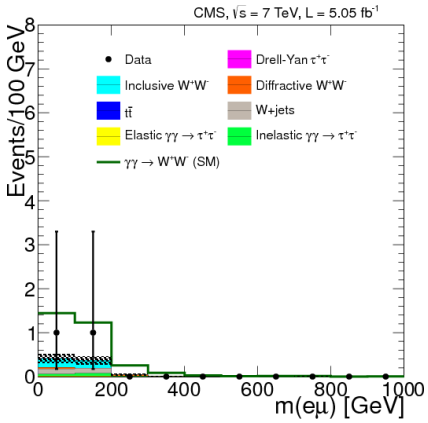


Figure 5: $\mu e$ invariant mass for events in the signal region with 0 extra tracks on the $\mu e$ vertex and $p_T(\mu e) > 30$ GeV. The backgrounds (solid histograms) are stacked with statistical uncertainties indicated by the shaded region, the signal histogram (open histogram) is stacked on top of the backgrounds.

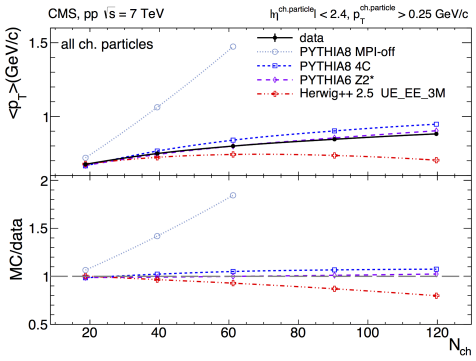


Figure 6: Mean transverse momentum of inclusive charged tracks with $p_T > 0.25$ GeV/c versus the corrected charged-particle multiplicity ($N_{ch}$ within $|\eta| < 2.4$).

production rate, or discrepancies in the kinematic distributions of multiple final state particles. A search for exclusive or quasi-exclusive $W^+W^-$ production by photon-photon interactions, $pp \to p^{(\star)}W^+W^-p^{(\star)}$, at $\sqrt{s} = 7$ TeV is reported using data collected by the CMS detector with an integrated luminosity of 5.05 fb$^{-1}$. Events are selected by requiring a $\mu^{\pm}e^{\mp}$ vertex with no additional associated charged tracks and dilepton transverse momentum $p_T(\mu^{\pm}e^{\mp}) > 30$ GeV. Two events passing all selection requirements are observed in the data, compared to a standard model expectation of $2.2 \pm 0.4$ signal events with $0.84 \pm 0.15$ background (Fig. 5). The tail of the dilepton $p_T$ distribution is studied for deviations from the standard model. No events are observed with $p_T > 100$ GeV. Model independent upper limits are computed and compared to predictions involving anomalous quartic gauge couplings [7].

## 4. Underlying events, MPI and DPS

In a proton-proton scattering the hadronic final state can be described as the superposition of different contributions. Most of the inelastic particle production can be described in a picture where an event is a combination of hadronic jets, originating from hard parton-parton interactions with exchanged momenta above several GeV/c and of an underlying event, which, consists of softer parton-parton interactions and of proton remnants. The underlying event (UE) is commonly defined as the set of all final-state particles that are not associated with the initial hard-parton scattering. This component is presumably dominated by perturbative (mini)jets with relatively small transverse momenta of a few GeV/c, produced in softer multi-parton interactions (MPI) as well as by soft hadronic strings from the high-rapidity remnants.

Multi-particle production in proton-proton collisions at $\sqrt{s} = 7$ TeV are studied as a function of the charged-particle multiplicity, $N_{ch}$ [8]. The produced particles are separated into two classes: those belonging to jets and those belonging to the underlying event. Charged particles are measured with pseudorapidity $|\eta| < 2.4$ and transverse momentum $p_T > 0.25$ GeV/c. Jets are reconstructed from charged particles only and having $p_T > 5$ GeV/c. The distributions of jet $p_T$, average $p_T$ of charged particles belonging to the underlying event or to jets, jet rates, and jet shapes are presented as functions of $N_{ch}$ and compared to the predictions of the PYTHIA and HERWIG event generators. Fig. 6 shows the distribution of mean transverse momentum of inclusive charged tracks versus the corrected pp charged-particle multiplicity. Current event generators tuned to reproduce the inelastic LHC data cannot describe within a single approach the dependence of various quantities on event multiplicity. For increasing $N_{ch}$, PYTHIA systematically predicts higher jet rates and harder $p_T$ spectra than seen in the data, whereas HERWIG shows the opposite trends. Predictions of PYTHIA without multi-parton interactions fail completely to describe the $N_{ch}$ dependence observed in the data, which demonstrate that MPI mechanism is criti-

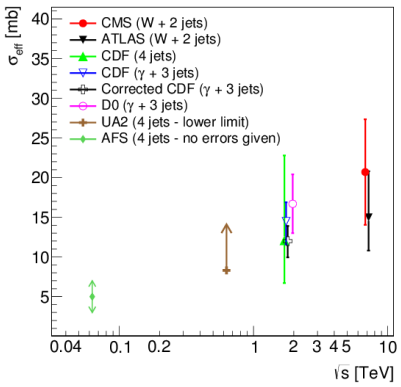


Figure 7: Center of mass energy dependence of $\sigma_{eff}$ measured by different experiments using different processes.

cal for reproducing the measured properties of the jets and UE for moderate and large charged-particle multiplicities. At the highest multiplicity, the data-model agreement is worse for most observables, indicating the need for further tuning and/or new model ingredients.

LHC probes small values of the momentum fraction $x$ carried by the colliding partons and the large densities at small-x values increase the probability of having two simultaneous parton-parton scatterings producing two independently identifiable hard scatterings in a single interaction. A study of double parton scattering (DPS) has been performed [9] with W+2-jet events, using 5 fb$^{-1}$ of the data at $\sqrt{s} = 7$ TeV. DPS with a W+2-jet final state occurs when one hard interaction produces a W boson and another produces a dijet in the same pp collision. Events with a W boson, reconstructed from the muon of $p_T > 35$ GeV and the missing transverse energy of $\not{E}_T > 30$ GeV, were required to have exactly two jets with $p_T > 20$ GeV and $|\eta| < 2$. Several observables, which are sensitive to discriminate DPS events from the Single Parton Scattering (SPS) ones, $\Delta\phi$, $\Delta^{rel}\ p_T$ and $\Delta S$ (as defined in [9]), have been studied. Corrected distributions are compared with particle level predictions of MADGRAPH MC sample. The effective DPS cross section, $\sigma_{eff}$, has been measured using a relation $\sigma_{eff} = R.\sigma_{2j}/f_{\rm DPS}$, where, $R = N_{W+0j}/N_{W+2j}$, and $\sigma_{2j}$ are the ratio of W+0-jet to W+2-jet events and the di-jet production cross section, respectively; $f_{\rm DPS}$ is the fraction of DPS events in the W+2-jet sample. The fraction of DPS in W + 2-jet events is extracted with a DPS + SPS template fit to the distribution of the $\Delta^{rel}p_T$ and $\Delta$S observables. The obtained value of the DPS fraction is

$$f_{DPS} = 0.055 \pm 0.002(\text{stat.}) \pm 0.014(\text{syst.})$$

and the effective cross section, characterizing the effective transverse area of hard partonic interactions in collisions between protons, is calculated to be

$$\sigma_{eff} = 20.7 \pm 0.8(\text{stat.}) \pm 6.6(\text{syst.})\text{mb}.$$

The measured value of the effective cross section is consistent with the Tevatron and ATLAS results (Fig. 7) .

## 5. Summary and outlook

In this paper, several achievements are being presented in the experimental search for diffractive, exclusive and underlying events at the LHC. Excellent experimental measurement of separated SD and DD cross-sections are being reported and compared with revised PYTHIA version based on a renormalised Regge theory model. The results from the first combined measurement by the CMS+TOTEM collaborations of the pseudorapidity distribution of charged particles at 8 TeV are discussed, and are compared to models and to lower energy measurements. In CEP process, with two candidates on $\gamma\gamma \to W^+W^-$ process, the best limits on the anomalous quartic couplings is extracted. The effective cross section for DPS, measured with CMS, are also found to be consistent with other experimental results.

The results presented in this paper provide the evidence for the excellent performance of CMS experiment and its potential for future measurements of diffractive, exclusive and soft QCD physics.

## References

[1] S. Chatrchyan et al., The CMS experiment at the CERN LHC, JINST, **3**, S08004 (2008).
[2] CMS Collaboration, CMS-PAS-FSQ-12-005.
[3] R. Ciesielski, K. Goulianos, arXiv:1205.1446.
[4] CMS and TOTEM Collaboration, arXiv:1405.0722.
[5] CMS Collaboration, JHEP **01**, 052 (2012).
[6] CMS Collaboration, JHEP **11**, 080 (2012).
[7] CMS Collaboration, JHEP **07**, 116 (2013).
[8] CMS Collaboration, Eur. Phys. J. **C73**, 2674 (2013).
[9] CMS Collaboration, JHEP **03**, 032 (2014). .